GBE

Chromosome-Scale Reference Genome Assemblies for Two *Anoplophora* Longhorned Beetle Species (Coleoptera: Cerambycidae)

Sangil Kim [1,2,*], Seunghun Jung [1], Brian D. Farrell [2], Seunggwan Shin [1,*]

[1]School of Biological Sciences and Research Institute of Basic Sciences, Seoul National University, Seoul 08826, Republic of Korea
[2]Museum of Comparative Zoology and Department of Organismic and Evolutionary Biology, Harvard University, Cambridge, MA 02138, USA

*Corresponding authors: Emails: sikim@g.harvard.edu; sk83@snu.ac.kr.

Accepted: March 03, 2026

Abstract

The Asian longhorned beetle, *Anoplophora glabripennis* (Motschulsky), and the citrus longhorned beetle, *A. malasiaca* (Thomson) (Coleoptera: Cerambycidae), represent two globally notorious forest pests whose introductions into North America and Europe have caused extensive damage to economically important temperate deciduous hardwood forests. *Anoplophora glabripennis* was the first longhorned beetle for which a reference genome was generated; however, the available assembly remains at the scaffold level, limiting chromosome-level analyses in a species that has emerged as a key model for investigating the genomic and ecological basis of plant-feeding evolution. Here, we present the first chromosome-scale genome assemblies for *A. glabripennis* and *Anoplophora malasiaca*, generated using PacBio HiFi long-read and Pore-C chromatin conformation capture sequencing. The assembled genomes span 730.1 and 708.0 Mbp for *A. glabripennis* and *A. malasiaca*, respectively, with scaffold N50 of 81.3 and 43.9 Mbp. A total of 96.7% and 95.2% of each assembly was anchored to 10 and 15 chromosome-level scaffolds, respectively, and the X chromosome was identified through synteny analysis. Repeat elements account for 66.5% and 65.5% of the genomes, and 14,624 and 13,814 protein-coding genes were functionally annotated. These reference-quality genomes provide a valuable comparative framework for elucidating the genomic basis of xylophagy and temperate adaptation in longhorned beetles and establish a foundation for devising targeted management strategies against invasive populations of both *A. glabripennis* and *A. malasiaca* in their introduced regions.

Key words: Asian longhorned beetle, citrus longhorned beetle, genome assembly, Pore-C contact map, synteny, plant cell wall-degrading enzymes.

Significance

Nearly a decade after the genome of the first longhorned beetle, *Anoplophora glabripennis*, was published, this globally invasive species has remained represented by a scaffold-level assembly, with genomic resources for Cerambycidae still limited. We present the chromosome-scale genome assemblies for *A. glabripennis* and its congener *A. malasiaca*, two of the most destructive invasive wood-boring insects in temperate forests of the Northern Hemisphere. These high-quality reference genomes enable chromosome-scale insights into the evolution of xylophagy and temperate adaptation in longhorned beetles and, by revealing a marked increase in chromosome numbers in *A. malasiaca*, provide a powerful system for investigating the role of chromosomal evolution and genome structural variation in adaptive evolution.

Introduction

Longhorned beetles (family Cerambycidae) constitute one of the most species-rich beetle families, comprising over 36,000 described species across 4,100 genera worldwide (Svacha and Lawrence 2014; Monné et al. 2017). Most longhorned beetles feed on plant tissues, and their remarkable species diversity is often explained by coevolutionary adaptive radiation associated with the rise and ecological dominance of flowering plants since the Cretaceous (Farrell 1998; McKenna et al. 2015; Zhang et al. 2018b; McKenna et al. 2019). The Asian longhorned beetle, *Anoplophora glabripennis*, and the citrus longhorned beetle, *A. malasiaca*, are among the most extensively studied species of longhorned beetles due to their status as global invasive wood-boring pests, whose introduction into deciduous forests of North America and Europe has inflicted substantial damage to a wide range of hardwood trees (Meng et al. 2015; Haack 2017). The successful establishment of these beetles in their introduced habitat is often attributed to their exceptionally wide host range, which likely involved specialized physiological and metabolic adaptations to circumvent defensive phytochemicals (Mason et al. 2016), as well as to efficiently digest and absorb nutrients from recalcitrant woody tissues (Shin et al. 2021, 2022). *Anoplophora glabripennis* has been established as a model system for studying digestive physiology and detoxification of xylophagous beetles (Scully et al. 2013a, 2013b, 2014, 2018; Mason et al. 2016), with its genome representing the first longhorned beetle genome to be sequenced and assembled (McKenna et al. 2016). Despite remaining at a fragmented scaffold-level, the reference genome of *A. glabripennis* has served as a foundational genomic resource for nearly a decade, garnering over 300 citations to date. Subsequent transcriptomic and genomic studies leveraging this reference genome uncovered horizontally acquired plant cell wall-degrading enzymes in the glycoside hydrolase families that most likely facilitated nutrient acquisition from woody plant tissues (Kirsch et al. 2014; McKenna et al. 2016; Shin et al. 2021, 2022).

The exceptional ability of *A. glabripennis* and *A. malasiaca* to establish in introduced habitats is also possibly associated with their early entry into temperate forests in East Asia, where they must routinely withstand cold and dry winter conditions. One strategy by which insects have evolved to survive unfavorable winter conditions is diapause, a hormonally-regulated, programed dormancy (Denlinger 2002), which can be particularly advantageous for invasive species by enabling persistence in novel environments that may present phenological mismatch or unusual climatic stress (Mahdjoub and Menu 2008; Sherpa et al. 2019; Torson et al. 2021). Diapause has been documented in *A. glabripennis* (Torson et al. 2021), together with additional adaptive mechanisms, such as specialized glycerol metabolism associated with cold tolerance (Xu et al. 2024). Despite these insights, our understanding of the genomic basis of temperate adaptation in *Anoplophora*, and phytophagous beetles at large, remains far from complete. A recent phylogenomic study further revealed that *A. glabripennis* and *A. malasiaca* independently expanded their range into temperate regions during the late Pliocene and Pleistocene, respectively, from within a predominantly subtropical lineage (Kim and Farrell 2025). Given their independent evolutionary trajectories toward temperate adaptation, enabled by their broad host ranges, the genomes of *A. glabripennis* and *A. malasiaca* provide an exceptional opportunity to investigate the genetic mechanisms underlying important life history traits through the lens of convergent evolution in harsh temperate environments.

In this study, we present the first chromosome-scale genome assemblies for *A. glabripennis* and *A. malasiaca*, providing a timely update to genomic resources for Cerambycidae. The new *A. glabripennis* genome not only improves upon the original reference genome assembly (Agla_2.0; GenBank accession no.: GCF_000390285.2), but it also represents a rare native Korean population of *A. glabripennis*, often referred to as the Korean morph or form *nobilis* sensu Lingafelter

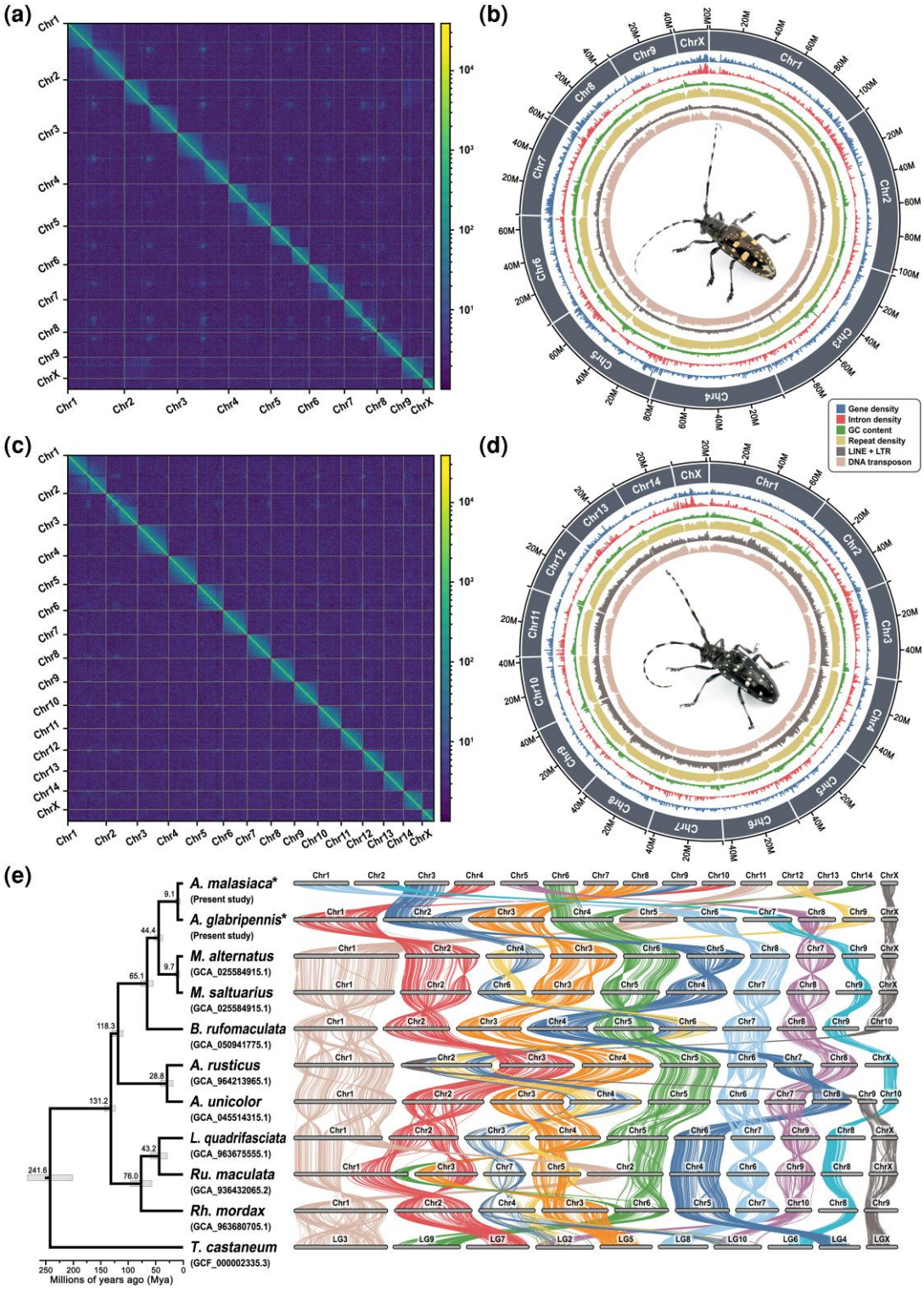

Fig. 1. Genomic characteristics of *Anoplophora glabripennis* and *A. malasiaca*. a, c) Hi-C contact frequency heatmaps (Pore-C) of the *A. glabripennis* (a) and *A. malasiaca* (c) genomes, illustrating chromosomal interactions and scaffold continuity across the 10 and 15 pseudo-chromosomes, respectively. b, d) Circular genome plots of *A. glabripennis* (b) and *A. malasiaca* (c), with inner tracks depicting key genomic features, and photographs of the corresponding voucher specimens shown at the center. e) Time-calibrated phylogeny and macrosynteny across the genomes of two *Anoplophora* species and eight representative cerambycid taxa, with *Tribolium castaneum* (Tenebrionidae) as an outgroup. Chromosome nomenclature for reference species corresponds to their respective NCBI genome assemblies.

and Hoebeke (2002), that is morphologically distinct and exhibits narrower host preferences than invasive populations established in urban habitats across East Asia, North America, and Europe (Williams et al. 2004; Lee et al. 2020). Together with the genome assembly of *A. malasiaca*, these genomic resources enable explicit tests of how gene family evolution and genome structural variation, acting across independent adaptive histories, have shaped host use, temperate adaptation, and evolutionary divergence at both species and population levels in this iconic model lineage of phytophagous beetles.

Results and Discussion

Genome Assembly

Genome assemblies were generated for the native Korean population of the Asian longhorned beetle (*Anoplophora glabripennis*; the Korean morph or form nobilis sensu Lingafelter and Hoebeke 2002) and for the citrus longhorned beetle (*A. malasiaca*) (Fig. 1), based on 31.9× and 25.3× coverage PacBio HiFi long-read sequence data. Each PacBio Sequel IIe flowcell yielded 23.7 and 17.9 Gbp of HiFi reads for the two species (Table S1). Initial genome assemblies based on the PacBio HiFi read, after resolving haplotypic duplications, resulted in 571 and 247 primary contigs with N50 of 11.7 and 11.9 Mbp for *A. glabripennis* and *A. malasiaca*. Contamination screening identified 179 contigs in *A. glabripennis* and three contigs in *A. malasiaca* as putative bacterial or fungal contaminants or as sequences with atypical GC content for arthropod genomes (Fig. S1); these contigs were, therefore, removed prior to subsequent scaffolding (Fig. S3). Chromosome-scale scaffolds were constructed by integrating the curated primary contigs with Pore-C chromatin conformation capture data, comprising 18.3 and 24.0 Gbp of Oxford Nanopore Technologies PromethION reads (Phred Q-score $\geq$ 10) for *A. glabripennis* and *A. malasiaca*, respectively (Table S1). This approach produced 265 and 73 final scaffolds, which were respectively anchored into 10 (*A. glabripennis*) and 15 pseudo-chromosomes (*A. malasiaca*) (Fig. 1a and c), consistent with previous karyotypic and cytogenic data (Ehara 1956; Abe et al. 1971a, 1971b; Liu et al. 2010). The final genome assemblies spanned 730.1 Mbp for *A. glabripennis*, and 708.0 Mbp for *A. malasiaca*, only slightly larger than the corresponding *k*-mer-based genome size estimates of 727.3 and 662.8 Mbp (Fig. S2). The assemblies showed scaffold N50 values of 81.3 and 43.8 Mbp, GC contents of 33.3% and 33.2% (Table 1), and BUSCO (Benchmarking Universal Single-copy Orthologs) completeness of 99.0% and 99.7% (Fig. S4; Table S6), with only 0.7% and 0.6% of duplicated genes, respectively, both exceeding the 90% benchmark recommended for reference-quality genomes (Lewin et al. 2018). Remapping of raw PacBio HiFi reads to the final assemblies yielded mapping rates of 98.2% and 99.9%, and assembly quality values of 41.0 and 40.0 (Table S3), confirming the high contiguity and accuracy of both genomes. In addition, complete mitochondrial genomes were assembled for the two species, each represented by a circularized sequence of 15,776 bp (*A. glabripennis*) and 14,786 bp (*A. malasiaca*) in length, both comprising 13 protein-coding genes, 22 tRNAs and two rRNA genes (Fig. S8).

Repeat Elements and Gene Annotations

Repetitive regions and transposable elements (TEs) in the *A. glabripennis* and *A. malasiaca* genomes were identified using a combination of homology-based and de novo prediction approaches. Repeat elements comprised 65.3% (461.1 Mbp) and 63.8% (430.3 Mbp) of the respective genomes, proportions well within the typical range reported for Cerambycidae (61.7% in *Rhagium mordax* to 81.8% in *Rutpela maculata*), with *Batocera rufomaculata* representing a notable outlier (Table S4). In both genomes, repetitive landscapes were dominated by unclassified repeats and DNA transposons, accounting for 47.4% and 33.0% of repetitive content in *A. glabripennis*, and 46.9% and 35.0% in *A. malasiaca*, respectively (Fig. S6). Telomeric repeats consisting of the canonical insect telomere motif $(TTAGG)_n$ were detected at either one or both ends of chromosomes 2, 4, 5, 6, and 9 in *A. glabripennis*, and of chromosomes 1, 2, 4, 5, 7, 8, 9, 11, 12, and X in *A. malasiaca* (Fig. S7). Given the documented variability of telomeric motifs in beetles, particularly in species-rich groups such as Cerambycidae (Prušáková et al. 2021), as well as the recent discovery of an unusual telomeric motif $(TTTGG)_n$ in the closely related leaf beetle family Chrysomelidae (Rico-Porras et al. 2025), further experimental validation is warranted to determine whether the chromosomal termini lacking detectable telomeric repeats in our assemblies are truly telomere-free, harbor previously uncharacterized telomeric motifs, or instead reflect scaffolding artifacts. Gene prediction and annotation identified 23,268 genes in *A. glabripennis* and 23,515 in *A. malasiaca*, of which 14,624 and 13,814 genes, respectively, were functionally annotated (Table 1 and Table S5). Gene models supported by species-specific transcriptomic and protein evidence derived from publicly available multitissue transcriptome data for each species yielded annotation sets comparable to the scaffold-level reference genome of *A. glabripennis* (Agla_2.0; 15,991 annotated genes) (McKenna

Table 1 Summary statistics for genome assemblies and annotations of *Anoplophora glabripennis* and *A. malasiaca*, together with those of eight additional longhorned beetles (Cerambycidae) and *Tribolium castaneum* (Tenebrionidae)

…	Anoplophora glabripennis	Anoplophora malasiaca	Monochamus alternatus	Monochamus saltuarius	Batocera rufomaculata	Arhopalus rusticus	Arhopalus unicolor	Leptura quadrifasciata	Rutpela maculata	Rhagium mordax	Tribolium castaneum
Assembly size (Mbp)	730.13	707.97	792.14	682.22	338.08	1,275.13	1,268.11	1,403.96	2,021.58	775.65	165.94
Total chromosome size (Mbp)	705.71	674.34	778.17	655.56	337.30	1,212.73	1,224.89	1,398.10	2,008.95	771.50	147.63
No. contigs	571	247	43	6,669	154	1,933	153	485	1,046	515	175
No. scaffolds	265	73	37	6,125	13	1,576	154	59	166	69	2,082
No. chromosomes	10	15	10	10	10	9	10	10	10	10	10
N50 (Contigs) (Mbp)	11.73	11.90	82.97	4.65	16.60	8.69	19.30	5.39	4.27	2.86	16.19
N50 (Scaffolds) (Mbp)	81.29	43.91	82.97	73.69	37.03	159.24	161.70	166.35	187.01	80.11	15.27
GC contents (%)	33.33	33.21	32.34	33.21	33.38	32.35	32.40	34.30	33.69	32.93	33.86
Predicted protein-coding genes	23,268	23,515	20,893	21,085	16,939	29,839	31,042	34,385	35,522	31,241	12,227
Annotated protein-coding genes	14,624	13,814	13,049	13,247	8,917	18,425	17,911	21,377	22,963	19,218	10,729
Protein-coding region content (%)	4.19	4.16	3.22	3.79	6.38	2.80	2.70	2.94	2.06	5.20	11.43
Mean gene length (bp)	10,431.18	9,556.91	11,409.58	10,347.66	10,494.68	13,187.25	9,065.88	11,259.13	16,694.45	6,448.64	7,044.49
Mean CDS length (bp)	1,270.09	1,191.65	1,200.61	1,177.47	1,269.70	1,142.27	1,068.50	1,200.35	1,172.68	1,281.58	1,551.67
Mean exon length (bp)	288.78	275.45	269.10	271.29	257.87	302.29	296.70	346.14	354.63	334.30	295.14
Mean intron density	3.76	3.69	3.89	3.77	4.30	3.33	2.88	2.90	3.00	3.19	4.66
Mean intron length (bp)	2,695.88	2,514.91	2,945.01	2,740.33	2,351.04	4,333.68	3,073.29	4,068.47	6,722.75	1,818.00	1,338.97
Repeat contents (%)	65.35	63.82	68.47	66.28	30.09	74.13	73.12	75.94	81.89	62.60	28.97
No. monoexonic genes	2,228	2,329	2,285	2,348	1,463	4,964	2,977	5,046	8,221	3,450	1,055
No. multiexonic genes	21,040	21,186	18,593	18,713	15,476	24,875	28,065	29,310	27,285	27,765	11,172
Ratio mono-/multiexonic genes	0.11	0.11	0.12	0.13	0.09	0.20	0.11	0.17	0.30	0.12	0.09
Total mRNA length (bp)	242,712,798	224,730,817	238,380,414	218,180,300	177,769,357	393,464,388	281,391,886	387,145,225	593,020,150	201,461,845	86,133,007
Total exon length (bp)	29,552,502	28,021,743	25,084,350	24,826,912	21,507,399	33,971,394	33,056,448	41,273,885	41,655,927	40,037,921	18,972,258
Total intron length (bp)	213,160,296	196,709,074	213,111,565	193,140,052	156,261,958	359,327,168	248,173,938	345,449,480	551,072,091	161,076,058	67,160,749

et al. 2016), and largely consistent with other published cerambycid genomes (Table 1; Fig. S4). Completeness of the annotated gene sets, assessed using BUSCO, recovered 96.7% (94.9% single-copy, 1.8% duplicated) for *A. glabripennis* and 96.3% (94.3% single-copy and 2.0% duplicated) for *A. malasiaca* (Fig. S4; Table S6), indicating highly complete gene annotations.

Synteny-Based Identification of Sex Chromosomes and Phylogenomic Inference

Synteny analyses revealed strong conservation of the X chromosome across all ten Cerambycidae species examined, as well as *Tribolium castaneum*, consistent with previous reports of exceptional X chromosome conservation in Coleoptera (Fu et al. 2022). This conserved macrosynteny pattern enabled the identification of chromosome 10 in *A. glabripennis* and 15 in *A. malasiaca* as the X chromosome (Fig. 1e). In addition to sex chromosome assignment, synteny analyses revealed extensive chromosomal restructuring associated with an increase in chromosome number from the putative ancestral karyotype of 10 chromosomes in Cerambycidae to 15 chromosomes in *A. malasiaca* (Fig. 1e). Specifically, chromosomes 1, 4, and 5 in *A. glabripennis* underwent fission, each giving rise to a pair of chromosomes in *A. malasiaca*: $Chr1_{Agla}$ to $Chr4_{Achi}$ and $Chr10_{Achi}$; $Chr4_{Agla}$ to $Chr6_{Achi}$ and $Chr14_{Achi}$; and $Chr5_{Agla}$ to $Chr11_{Achi}$ and $Chr13_{Achi}$. Our time-calibrated phylogeny based on genome-scale data confirms a sister relationship between *A. glabripennis* and *A. malasiaca*, which diverged approximately 9.1 Mya [95% highest posterior density (HPD): 5.6 to 13.2 Mya], closely matching a previous estimate of 8.5 Mya (95% HPD: 5.4 to 11.1 Mya) inferred from target enrichment phylogenomics with broader taxon sampling (Kim and Farrell 2025). The extent of chromosomal restructuring observed between these two species is remarkable given their recent divergence, and it may be associated with specialized adaptation to temperate environments within a lineage that originated in subtropical to tropical forests of Southeast Asia (Kim and Farrell 2025). Although elucidating the genetic basis of their temperate adaptation, characterized by broad host use across East Asia, and more recently, North America and Europe, is beyond the scope of this study, the magnitude of chromosomal reorganization observed likely has contributed to the maintenance of reproductive isolation between the two largely sympatric species, which may occasionally engage in mating behavior on the same host plants (Wang and Keena 2021; Qin et al. 2024). Indeed, differences in chromosome number between these two species may act as an intrinsic barrier to gene flow by generating hybrid sterility through meiotic segregation errors and dysfunctional gamete formation, or by suppressing recombination in heterokaryotypes (Ayala and Coluzzi 2005; Faria and Navarro 2010), a pattern well documented in butterflies (e.g. Lukhtanov et al. 2005; Talavera et al. 2013; Lucek 2018). Together, our genome-scale phylogenomic and synteny analyses establish a robust temporal framework for chromosomal evolution in *Anoplophora* and provide foundational genomic resources for comparative studies of chromosome-mediated reproductive isolation and the genetic basis of temperate adaptation and broad host use underlying exceptional invasiveness of these globally important forest pests.

Materials and Methods

Sample Collection

Adult specimens of *A. glabripennis* were collected in August 2021 from *Acer pictum* subsp. *mono* (Sapindaceae) in Bokjusan National Recreation Forest, Cheorwon-gun, Gangwon-do, Republic of Korea (38°8.664′N 127°28.544′E; elev. 522 m), and of *A. malasiaca* in September 2021 from *Salix koreensis* (Salicaceae) at Amsa Ecological Park along the Han River, Gangdong-gu, Seoul, Republic of Korea (37°33.325′N 127°7.376′E; elev. 11 m). Sampling and transfer of specimens for sequencing were conducted in compliance with applicable national laws and regulations of the Republic of Korea. All specimens were starved for several days to minimize contamination from gut contents, flash-frozen in liquid nitrogen, and cryo-preserved at −80 °C until extraction. For each species, a total of two specimens were used: One for PacBio sequencing and the other for Pore-C sequencing. All experiments involving insect specimens were conducted in accordance with the relevant guidelines and regulations governing the ethical use of animals in research, as overseen by the FAS Standing Committee on the Use of Animals in Research and Teaching at Harvard University (FAS IACUC; Assurance no. A3593-01).

Nucleic Acid Extraction and Sequencing

High molecular weight (HMW) genomic DNA (gDNA) was extracted from individual adult specimens (voucher nos.: MCZ-SK1106 and MCZ-SK1107) using the Qiagen Blood & Cell Culture DNA Kit with Genomic-tips 20/G (Qiagen, Hilden, Germany). DNA integrity was assessed by electrophoresis on a 1% agarose gel with a lambda DNA size standard, and concentration and purity were measured with a Quantus Fluorometer (Promega, Madison, WI, USA) and a Nanodrop Spectrophotometer (Thermo Fisher Scientific, Waltham, MA, USA). The extracted HMW gDNA were further enriched for long

fragments by removing DNA fragments <40 kbp with the Short Read Eliminator XL Kit (Pacific Biosciences, Menlo Park, CA, USA), and subsequently sheared to ~20 kbp with the Megaruptor 2 (Diagenode, Liège, Belgium). PacBio SMRT libraries were constructed using the SMRTbell Prep Kit 3.0, and sequenced on a single SMRT HiFi cell of the PacBio Sequel IIe system at the Brigham Young University DNA Sequencing Center (Provo, UT, USA). Chromatin conformation capture data were generated from additional individual specimens of *A. glabripennis* and *A. malasiaca* (voucher nos.: MCZ-SK1262 and MCZ-SK1256) following the Pore-C protocol (Deshpande et al. 2022). Briefly, chromatin structure within intact nuclei was fixed in situ with formaldehyde to preserve native three-dimensional chromatin interactions and subsequently permeabilized. After heat denaturation, chromatin was digested with the restriction enzyme *Nla*III (New England Biolabs, Ipswich, MA, USA), and proximally crosslinked DNA fragments were purified using phenol–chloroform extraction. The final Pore-C sequencing libraries were prepared using the Genomic DNA by Ligation Protocol (SQK-LSK114; Oxford Nanopore Technologies, Oxford, UK) and sequenced on individual PromethION flowcells at the National Instrumentation Center for Environmental Management, Seoul National University (Seoul, Republic of Korea).

Genome Assembly and Scaffolding

Genome size and heterozygosity for *A. glabripennis* and *A. malasiaca* were estimated from raw PacBio HiFi reads using Jellyfish v2.3.0 (Marçais and Kingsford 2011) with a k-mer size of 35 and GenomeScope v2.0 (Ranallo-Benavidez et al. 2020). De novo assembly of primary contigs was performed using Hifiasm v0.16.1 (Cheng et al. 2021), and putative allelic redundancies were subsequently resolved with Purge Haplotigs v1.1.2 (Roach et al. 2018). The primary contigs were screened using BlobTools v1.1.1 (Laetsch and Blaxter 2017) to identify and remove potential contaminant sequences prior to scaffolding. Chromosome-level scaffolds were generated by integrating the filtered primary contigs with Pore-C data using the Pore-C Snakemake workflow (Deshpande et al. 2022) and the 3D-DNA pipeline v180992 (Dudchenko et al. 2017). The Hi-C interaction maps were then inspected and manually curated in Juicebox v2.20.00 (Durand et al. 2016), after which scaffolds were finalized using 3D-DNA. Scaffold contiguity was further improved using RagTag v2.1.0 (Alonge et al. 2022), with the filtered primary contigs serving as the reference. Specifically, scaffolds generated from the final 3D-DNA assembly were used as queries, and any scaffolds artificially fragmented during Pore-C interaction-based scaffolding were rejoined by inserting stretches of "N" where supported by the filtered primary contigs of the respective species. This resulted in a reduction in scaffold numbers from 292 to 265 in *A. glabripennis* and from 104 to 75 in *A. malasiaca*, while the mean scaffold length increased from 2.50 to 2.76 Mbp and from 6.81 to 9.33 Mbp, respectively. Residual assembly errors were corrected in a final polishing step using Inspector v1.3.1 (Chen et al. 2021) based on the original raw PacBio HiFi reads. High-resolution Hi-C contact maps were rendered in HiGlass v0.8.0 (Kerpedjiev et al. 2018) to visualize overall chromosomal architecture. In addition, circular mitochondrial genomes for each species were constructed using the MitoHiFi pipeline v3.2 (Uliano-Silva et al. 2023), guided by the reference mitochondrial genome of *A. glabripennis* (GenBank accession no.: NC_008221.1). Final circular mitochondrial sequences were selected based on annotations generated by MitoFinder v1.4.1 (Allio et al. 2020) and visualized as circular genome maps using the Proksee server (Grant et al. 2023).

Repeat Element and Gene Annotations

Repeat regions and TEs in *Anoplophora glabripennis* and *A. malasiaca* genomes were identified and masked using the Earl Grey pipeline v4.4.0 (Baril et al. 2024). RepeatMasker v4.1.5 (Smit et al. 2023) was used to annotate repeats based on the Dfam v3.8 (Storer et al. 2021) TE database for Coleoptera, supplemented with species-specific de novo repeat libraries generated with RepeatModeler v2.0.5 (Flynn et al. 2020). De novo consensus TE sequences were curated through the BEAT process (Platt et al. 2016), and long terminal repeat retrotransposons were further annotated using LTR_Finder v1.07 (Xu and Wang 2007). Repeat landscape distributions were analyzed by calculating Kimura two-parameter substitution levels with calcDivergenceFromAlign.pl script in RepeatMasker, generating divergence-based repeat landscape plots. Telomeric repeats were additionally searched for using tidk v0.2.7 (Brown et al. 2025) with the canonical insect telomere motif $(TTAGG)_n$.

Based on repeat-masked genome assemblies, ab initio gene prediction was performed using BRAKER v3.0.7 (Gabriel et al. 2024), incorporating species-specific RNA sequencing and protein evidence, the Arthropoda OrthoDB v10 dataset (Kriventseva et al. 2019), and reference protein sets from *A. glabripennis* (GCF_000390285.2), *T. castaneum* (GCF_000002335.3), *Drosophila melanogaster* (GCF_000001215.4), and *Bombyx mori* (GCF_030269925.1). Species-specific RNA and protein datasets were generated from publicly available raw RNA sequencing data spanning multiple

developmental stages and tissue types for *A. glabripennis* (NCBI SRA accession nos: SRR1799851, SRR1799852, SRR2682325, SRR11357720) and *A. malasiaca* (SRR10297523–SRR10297528) (Table S2). All raw RNA sequencing reads were assembled using rnaSPAdes v3.13.0 (Bushmanova et al. 2019) and translated into amino acid sequences with TransDecoder v5.7.0 (Haas 2023) (Fig. S5; Table S2). Gene prediction was conducted with AUGUSTUS v3.5.5 (Stanke et al. 2008), using transcriptome-based training evidence from GeneMark-ET v4.72 (Lomsadze et al. 2005) and protein-based training evidence from GeneMark-EP + v4.72 (Brůna et al. 2020). Consensus gene models were generated by integrating a total of seven independent prediction runs for each species using TSEBRA v1.1.1 (Gabriel et al. 2021). To avoid misinterpreting alternative isoforms as potential rearrangement events, only the longest isoform per gene was retained for downstream analyses. Finally, functional annotation was performed using eggNOG-mapper v2.1.12 (Cantalapiedra et al. 2021) based on the Insecta eggNOG database.

Synteny-Based Identification of the X Chromosome

Genome synteny was analyzed across the genome assemblies of *A. glabripennis*, *A. malasiaca*, and eight additional species of Cerambycidae, with *Tribolium castaneum* (Tenebrionidae) included as an outgroup. Orthologous genes were identified via reciprocal-best BLASTp (Altschul 1997) hits among annotated proteins using DIAMOND v2.0.13 (Buchfink et al. 2021). Chromosomal homology was subsequently evaluated using Bonferroni-corrected one-sided Fisher's exact tests implemented in odp v0.3.3 (Schultz et al. 2023). Conserved macrosyntenic blocks were visualized as ribbon diagrams following the odp_nway_rbh pipeline within odp, with linkage groups on each chromosome of the *A. glabripennis* genome manually assigned the same color to improve the visualization of synteny. Given the high level of X chromosome conservation across Coleoptera (Fu et al. 2022), the X chromosomes in our newly assembled *Anoplophora* genomes were identified as those syntenic to the X chromosomes of other genomes examined.

Orthologous Gene Identification and Phylogenomic Inference

Orthologous genes and orthogroups across the ten Cerambycidae and *T. castaneum* genomes were identified using OrthoFinder v2.5.5 (Emms and Kelly 2019), with DIAMOND for sequence alignment and FastTree v2.1.11 (Price et al. 2010) for initial maximum likelihood (ML) tree inference. A total of 3,006 single-copy orthologs were identified, aligned with MAFFT v7.5.26 (Katoh and Standley 2013), and trimmed with trimAl v1.4 (Capella-Gutiérrez et al. 2009) under the gappyout algorithm. ML gene trees for each ortholog were inferred using IQ-TREE v2.2.2.6 (Minh et al. 2020) with the MFP + MERGE option. The species tree was reconstructed under the multispecies coalescent model using ASTRAL v5.7.8 (Zhang et al. 2018a), with *T. castaneum* as the outgroup. Divergence times were estimated within a Bayesian framework using MCMCtree implemented in PAML v4.10.7 (Yang 2007), employing the approximate likelihood calculation method and two calibration points: (i) a fossil calibration for crown-group Cerambycidae, representing the divergence between *Anoplophora* (subfamily Lamiinae) and the subfamily Lepturinae based on †*Cretoprionus liutiaogouensis* Wang et al. from the Lower Cretaceous (ca. 122.5 to 124.0 Mya; Wang et al. 2014); and (ii) a secondary calibration for the Cerambycidae–Tenebrionidae divergence at approximately 220.2 Mya (95% HPD: 188.1 to 237.6 Mya) (McKenna et al. 2019).

Supplementary Material

Supplementary material is available at *Genome Biology and Evolution* online.

Acknowledgments

We express our gratitude to Bokjusan National Recreational Forest (Korea Forest Service) and Amsa Ecological Park (Seoul Metropolitan Government) for granting permission to collect specimens of *Anoplophora glabripennis* and *A. malasiaca*. Computational analyses were performed on the FASRC Cannon cluster at Harvard University. This work was supported by the National Research Foundation of Korea (NRF) grant (MEST, 2019R1A6A1A10073437; MSIT, RS-2021-NR061223; SRC, RS-2021-NR060088); the National Institute of Biological Resources, Ministry of Environment (MOE) (NIBR202206103; NIBR202305101; NIBR202405101; NIBR202505101; NIBR202605103); the Graduate Research Fund of the Department of Organismic and Evolutionary Biology, Harvard University, and the Putnam Expedition Grant from the Museum of Comparative Zoology, Harvard University.

Author Contributions

S.K.: Conceptualization; data curation; formal analysis; funding acquisition; investigation; methodology; project administration; resources; validation; visualization; writing—original draft; writing—review and editing. S.J.: Formal analysis; methodology; visualization. B.D.F.: Conceptualization; funding acquisition; investigation; project administration; resources; supervision; writing

—review and editing. S.S.: Funding acquisition; project administration; resources; supervision; writing—review and editing.

Conflict of Interest

The authors declare no competing interests.

Data Availability

All raw sequencing data (PacBio HiFi and Pore-C) and the final genome assemblies for *A. glabripennis* and *A. malasiaca* have been deposited in NCBI BioProject PRJNA1393341. PacBio HiFi sequencing data and Pore-C sequencing data are available within the NCBI Sequence Read Archive (SRA) (https://www.ncbi.nlm.nih.gov/sra) under accession numbers SRR36592619–SRR36592622. The final chromosome-scale genome assemblies have been deposited in GenBank under accession numbers GCA_054644005.1 and GCA_054644075.1. The whole genome assembly and annotation files are available from the Figshare Repository (https://doi.org/10.6084/m9.figshare.30938984.).

Literature Cited

Abe A, Kudoh K, Saitoh K. Chromosome numbers of 20 species of Cerambycid beetles (Coleoptera). Chromosome Inf Serv. 1971a:12:11–12.

Abe A, Kudoh K, Saitoh K. Chromosome studies of beetles. III. A chromosome survey of 18 species of the subfamily Lamiinae (Cerambycidae). Sci Rep Hirosaki Univ. 1971b:18:53–63.

Allio R, et al. MitoFinder: efficient automated large-scale extraction of mitogenomic data in target enrichment phylogenomics. Mol Ecol Resour. 2020:20:892–905. https://doi.org/10.1111/1755-0998.13160.

Alonge M, et al. Automated assembly scaffolding using RagTag elevates a new tomato system for high-throughput genome editing. Genome Biol. 2022:23:1–19. https://doi.org/10.1186/s13059-022-02823-7.

Altschul S. Gapped BLAST and PSI-BLAST: a new generation of protein database search programs. Nucleic Acids Res. 1997:25:3389–3402. https://doi.org/10.1093/nar/25.17.3389.

Ayala FJ, Coluzzi M. Chromosome speciation: humans, *Drosophila*, and mosquitoes. Proc Natl Acad Sci U S A. 2005:102:6535–6542. https://doi.org/10.1073/pnas.0501847102.

Baril T, Galbraith J, Hayward A. Earl Grey: a fully automated user-friendly transposable element annotation and analysis pipeline. Mol Biol Evol. 2024:41:msae068. https://doi.org/10.1093/molbev/msae068.

Brown MR, Manuel Gonzalez de La Rosa P, Blaxter M. Tidk: a toolkit to rapidly identify telomeric repeats from genomic datasets. Bioinformatics. 2025:41:btaf04. https://doi.org/10.1093/bioinformatics/btaf049.

Brůna T, Lomsadze A, Borodovsky M. GeneMark-EP+: eukaryotic gene prediction with self-training in the space of genes and proteins. NAR Gen Bioinf. 2020:2:lqaa026. https://doi.org/10.1093/nargab/lqaa026.

Buchfink B, Reuter K, Drost HG. Sensitive protein alignments at tree-of-life scale using DIAMOND. Nat Methods. 2021:18:366–368. https://doi.org/10.1038/s41592-021-01101-x.

Bushmanova E, Antipov D, Lapidus A, Prjibelski AD. rnaSPAdes: a *de novo* transcriptome assembler and its application to RNA-Seq data. GigaScience. 2019:8:giz100. https://doi.org/10.1093/gigascience/giz100.

Cantalapiedra CP, Hernández-Plaza A, Letunic I, Bork P, Huerta-Cepas J. eggNOG-mapper v2: functional annotation, orthology assignments, and domain prediction at the metagenomic scale. Mol Biol Evol. 2021:38:5825–5829. https://doi.org/10.1093/molbev/msab293.

Capella-Gutiérrez S, Silla-Martínez JM, Gabaldón T. Trimal: a tool for automated alignment trimming in large-scale phylogenetic analyses. Bioinformatics. 2009:25:1972–1973. https://doi.org/10.1093/bioinformatics/btp348.

Chen Y, Zhang Y, Wang AY, Gao M, Chong Z. Accurate long-read de novo assembly evaluation with inspector. Genome Biol. 2021:22:312. https://doi.org/10.1186/s13059-021-02527-4.

Cheng H, Concepcion GT, Feng X, Zhang H, Li H. Haplotype-resolved de novo assembly using phased assembly graphs with hifiasm. Nat Methods. 2021:18:170–175. https://doi.org/10.1038/s41592-020-01056-5.

Denlinger DL. Regulation of diapause. Annu Rev Entomol. 2002:47:93–122. https://doi.org/10.1146/annurev.ento.47.091201.145137.

Deshpande AS, et al. Identifying synergistic high-order 3D chromatin conformations from genome-scale nanopore concatemer sequencing. Nat Biotechnol. 2022:40:1488–1499. https://doi.org/10.1038/s41587-022-01289-z.

Dudchenko O, et al. De novo assembly of the *Aedes aegypti* genome using Hi-C yields chromosome-length scaffolds. Science. 2017:356:92–95. https://doi.org/10.1126/science.aal3327.

Durand NC, et al. Juicebox provides a visualization system for hi-C contact maps with unlimited zoom. Cell Syst. 2016:3:99–101. https://doi.org/10.1016/j.cels.2015.07.012.

Ehara S. A comparative histology of male gonads in some cerambycid beetles with notes on the chromosomes. J Faculty Sci Hokkaido Univ Ser VI. 1956:12:309–316.

Emms DM, Kelly S. OrthoFinder: phylogenetic orthology inference for comparative genomics. Genome Biol. 2019:20:1–14. https://doi.org/10.1186/s13059-019-1832-y.

Faria R, Navarro A. Chromosomal speciation revisited: rearranging theory with pieces of evidence. Trends Ecol Evol. 2010:25:660–669. https://doi.org/10.1016/j.tree.2010.07.008.

Farrell BD. Inordinate fondness" explained: why are there so many beetles? Science. 1998:281:555–559. https://doi.org/10.1126/science.281.5376.555.

Flynn JM, et al. RepeatModeler2 for automated genomic discovery of transposable element families. Proc Natl Acad Sci U S A. 2020:117:9451–9457. https://doi.org/10.1073/pnas.1921046117.

Fu N, et al. Chromosome-level genome assembly of *Monochamus saltuarius* reveals its adaptation and interaction mechanism with pine wood nematode. Int J Biol Macromol. 2022:222:325–336. https://doi.org/10.1016/j.ijbiomac.2022.09.108.

Gabriel L, et al. BRAKER3: fully automated genome annotation using RNA-seq and protein evidence with GeneMark-ETP, AUGUSTUS, and TSEBRA. Genome Res. 2024:34:769–777. https://doi.org/10.1101/gr.278090.123.

Gabriel L, Hoff KJ, Brůna T, Borodovsky M, Stanke M. TSEBRA: transcript selector for BRAKER. BMC Bioinform. 2021:22:566. https://doi.org/10.1186/s12859-021-04482-0.

Grant JR, et al. Proksee: in-depth characterization and visualization of bacterial genomes. Nucleic Acids Res. 2023:51: W484–W492. https://doi.org/10.1093/nar/gkad326.
Haack RA. Feeding biology of cerambycids. In: Wang Q, editor. Cerambycidae of the world: biology and pest management. CRC Press; 2017. p. 105–124.
Haas BJ. 2023. TransDecoder (version 5.7.0). http://github.com/TransDecoder/TransDecoder.
Katoh K, Standley DM. MAFFT multiple sequence alignment software version 7: improvements in performance and usability. Mol Biol Evol. 2013:30:772–780. https://doi.org/10.1093/molbev/mst010.
Kerpedjiev P, et al. Higlass: web-based visual exploration and analysis of genome interaction maps. Genome Biol. 2018:19:125. https://doi.org/10.1186/s13059-018-1486-1.
Kim S, Farrell BD. Target enrichment museomics of the Asian longhorned beetle and its relatives (Cerambycidae: *Anoplophora*) reveals two independent origins of life in the cold. Syst Entomol. 2025:50:139–153. https://doi.org/10.1111/syen.12647.
Kirsch R, et al. Horizontal gene transfer and functional diversification of plant cell wall degrading polygalacturonases: key events in the evolution of herbivory in beetles. Insect Biochem Mol Biol. 2014:52:33–50. https://doi.org/10.1016/j.ibmb.2014.06.008.
Kriventseva EV, et al. OrthoDB v10: sampling the diversity of animal, plant, fungal, protist, bacterial and viral genomes for evolutionary and functional annotations of orthologs. Nucleic Acids Res. 2019:47:D807–D811. https://doi.org/10.1093/nar/gky1053.
Laetsch DR, Blaxter ML. BlobTools: interrogation of genome assemblies. F1000Res. 2017:6:1287–1287. https://doi.org/10.12688/f1000research.12232.1.
Lee S, Lee Y, Lee S. Population genetic structure of *Anoplophora glabripennis* in South Korea: invasive populations in the native range? J Pest Sci (2004). 2020:93:1181–1196. https://doi.org/10.1007/s10340-020-01245-3.
Lewin HA, et al. Earth BioGenome project: sequencing life for the future of life. Proc Natl Acad Sci U S A. 2018:115:4325–4333. https://doi.org/10.1073/pnas.1720115115.
Lingafelter SW, Hoebeke ER. Revision of *Anoplophora* (Coleoptera: Cerambycidae). Entomological Society of Washington; 2002.
Liu P, et al. Karyotypes of *Monochamus alternatus* and *Anoplophora glabripennis*. Chin Bull Entomol. 2010:47: 299–307. in Chinese.
Lomsadze A, Ter-Hovhannisyan V, Chernoff YO, Borodovsky M. Gene identification in novel eukaryotic genomes by self-training algorithm. Nucleic Acids Res. 2005:33:6494–6506. https://doi.org/10.1093/nar/gki937.
Lucek K. Evolutionary mechanisms of varying chromosome numbers in the radiation of *Erebia* butterflies. Genes (Basel). 2018:9:166. https://doi.org/10.3390/genes9030166.
Lukhtanov VA, et al. Reinforcement of pre-zygotic isolation and karyotype evolution in *Agrodiaetus* butterflies. Nature. 2005:436:385–389. https://doi.org/10.1038/nature03704.
Mahdjoub T, Menu F. Prolonged diapause: a trait increasing invasion speed? J Theor Biol. 2008:251:317–330. https://doi.org/10.1016/j.jtbi.2007.12.002.
Marçais G, Kingsford C. A fast, lock-free approach for efficient parallel counting of occurrences of k-mers. Bioinformatics. 2011:27: 764–770. https://doi.org/10.1093/bioinformatics/btr011.
Mason CJ, Scully ED, Geib SM, Hoover K. Contrasting diets reveal metabolic plasticity in the tree-killing beetle, *Anoplophora glabripennis* (Cerambycidae: Lamiinae). Sci Rep. 2016:6: 33813. https://doi.org/10.1038/srep33813.
McKenna DD, et al. The beetle tree of life reveals that Coleoptera survived end-Permian mass extinction to diversify during the Cretaceous terrestrial revolution. Syst Entomol. 2015:40: 835–880. https://doi.org/10.1111/syen.12132.
McKenna DD, et al. Genome of the Asian longhorned beetle (*Anoplophora glabripennis*), a globally significant invasive species, reveals key functional and evolutionary innovations at the beetle–plant interface. Genome Biol. 2016:17:227–227. https://doi.org/10.1186/s13059-016-1088-8.
McKenna DD, et al. The evolution and genomic basis of beetle diversity. Proc Natl Acad Sci U S A. 2019:116:24729–24737. https://doi.org/10.1073/pnas.1909655116.
Meng PS, Hoover K, Keena MA. Asian longhorned beetle (Coleoptera: Cerambycidae), an introduced pest of maple and other hardwood trees in North America and Europe. J Integr Pest Manag. 2015:6:1–13. https://doi.org/10.1093/jipm/pmv003.
Minh BQ, et al. IQ-TREE 2: new models and efficient methods for phylogenetic inference in the genomic era. Mol Biol Evol.2020:37:1530–1534. https://doi.org/10.1093/molbev/msaa015.
Monné ML, Monné MA, Wang Q. General morphology, classification, and biology of cerambycidae. In: Wang Q, editor. Cerambycidae of the world: biology and pest management. CRC Press; 2017. p. 1–70.
Platt RN, Blanco-Berdugo L, Ray DA. Accurate transposable element annotation is vital when analyzing new genome assemblies. Genome Biol Evol. 2016:8:403–410. https://doi.org/10.1093/gbe/evw009.
Price MN, Dehal PS, Arkin AP. FastTree 2—approximately maximum-likelihood trees for large alignments. PLoS One. 2010:5:e9490. https://doi.org/10.1371/journal.pone.0009490.
Prušáková D, et al. Telomeric DNA sequences in beetle taxa vary with species richness. Sci Rep. 2021:11:13319. https://doi.org/10.1038/s41598-021-92705-y.
Qin H, et al. Is there hybridization between 2 species of the same genus in sympatry? The genetic relationships between *Anoplophora glabripennis*, *Anoplophora chinensis*, and putative hybrids. Insect Sci. 2024:31:633–645. https://doi.org/10.1111/1744-7917.13256.
Ranallo-Benavidez TR, Jaron KS, Schatz MC. GenomeScope 2.0 and smudgeplot for reference-free profiling of polyploid genomes. Nat Commun. 2020:11:1432. https://doi.org/10.1038/s41467-020-14998-3.
Rico-Porras JM, Mora P, Palomeque T, Cabral-de-Mello DC, Lorite P. Comparative cytogenetics of *Lachnaia* species (Coleoptera: Chrysomelidae) reveals a novel telomeric motif (TTTGG) in insects. Organ Diver Evol. 2025:25:329–342. https://doi.org/10.1007/s13127-025-00676-z.
Roach MJ, Schmidt SA, Borneman AR. Purge Haplotigs: Allelic contig reassignment for third-gen diploid genome assemblies. BMC Bioinf. 2018:19:460. https://doi.org/10.1186/s12859-018-2485-7.
Schultz DT, et al. Ancient gene linkages support ctenophores as sister to other animals. Nature. 2023:618:110–117. https://doi.org/10.1038/s41586-023-05936-6.
Scully ED, et al. Metagenomic profiling reveals lignocellulose degrading system in a microbial community associated with a wood-feeding beetle. PLoS One. 2013a:8:e73827. https://doi.org/10.1371/journal.pone.0073827.
Scully ED, et al. Functional genomics and microbiome profiling of the Asian longhorned beetle (*Anoplophora glabripennis*) reveal insights into the digestive physiology and nutritional ecology of wood feeding beetles. BMC Genomics.

2014:15:1096–1096. https://doi.org/10.1186/1471-2164-15-1096.
Scully ED, et al. Host-plant induced changes in microbial community structure and midgut gene expression in an invasive polyphage (*Anoplophora glabripennis*). Sci Rep. 2018:8:9620. https://doi.org/10.1038/s41598-018-27476-0.
Scully ED, Hoover K, Carlson JE, Tien M, Geib SM. Midgut transcriptome profiling of *Anoplophora glabripennis*, a lignocellulose degrading cerambycid beetle. BMC Genomics. 2013b:14:850–850. https://doi.org/10.1186/1471-2164-14-850.
Sherpa S, et al. Unravelling the invasion history of the Asian tiger mosquito in Europe. Mol Ecol. 2019:28:2360–2377. https://doi.org/10.1111/mec.15071.
Shin NR, et al. Larvae of longhorned beetles (Coleoptera; Cerambycidae) have evolved a diverse and phylogenetically conserved array of plant cell wall degrading enzymes. Syst Entomol. 2021:46:784–797. https://doi.org/10.1111/syen.12488.
Shin NR, Doucet D, Pauchet Y. Duplication of horizontally acquired GH5-2 enzymes played a central role in the evolution of longhorned beetles. Mol Biol Evol. 2022:39:1–14. https://doi.org/10.1093/molbev/msac128.
Smit AFA, Hubley R, Green P. 2023. RepeatMasker Open-4.0. http://www.repeatmasker.org.
Stanke M, Diekhans M, Baertsch R, Haussler D. Using native and syntenically mapped cDNA alignments to improve *de novo* gene finding. Bioinformatics. 2008:24:637–644. https://doi.org/10.1093/bioinformatics/btn013.
Storer J, Hubley R, Rosen J, Wheeler TJ, Smit AF. The Dfam community resource of transposable element families, sequence models, and genome annotations. Mob DNA. 2021:12:2. https://doi.org/10.1186/s13100-020-00230-y.Svacha P, Lawrence JF. Cerambycidae latreille, 1802. In: Leschen RAB, Beutel RG, editors. Handbook of zoology. Vol. 3: Walter de Gruyter; 2014. p. 77–177.
Talavera G, Lukhtanov VA, Rieppel L, Pierce NE, Vila R. In the shadow of phylogenetic uncertainty: the recent diversification of *Lysandra* butterflies through chromosomal change. Mol Phylogenet Evol. 2013:69:469–478. https://doi.org/10.1016/j.ympev.2013.08.004.
Torson AS, et al. Dormancy in laboratory-reared Asian longhorned beetles, *Anoplophora glabripennis*. J Insect Physiol. 2021:130:104179. https://doi.org/10.1016/j.jinsphys.2020.104179.
Uliano-Silva M, et al. Mitohifi: a python pipeline for mitochondrial genome assembly from PacBio high fidelity reads. BMC Bioinformatics. 2023:24:288. https://doi.org/10.1186/s12859-023-05385-y.
Wang B, et al. The earliest known longhorn beetle (Cerambycidae: Prioninae) and implications for the early evolution of Chrysomeloidea. J Syst Palaeontol. 2014:12:565–574. https://doi.org/10.1080/14772019.2013.806602.
Wang X, Keena MA. Hybridization potential of two invasive Asian longhorn beetles. Insects. 2021:12:1139. https://doi.org/10.3390/insects12121139.
Williams DW, Lee HP, Kim IK. Distribution and abundance of *Anoplophora glabripennis* (Coleoptera: cerambycidae) in natural *Acer* stands in South Korea. Environ Entomol. 2004:33:540–545. https://doi.org/10.1603/0046-225X-33.3.540.
Xu Y, et al. Glycerol metabolism is important for the low-temperature adaptation of a global quarantine pest *glabripennis* larvae. J Agric Food Chem. 2024:72:17868–17879. https://doi.org/10.1021/acs.jafc.4c03896.
Xu Z, Wang H. LTR_FINDER: an efficient tool for the prediction of full-length LTR retrotransposons. Nucleic Acids Res. 2007:35:W265–W268. https://doi.org/10.1093/nar/gkm286.
Yang Z. PAML 4: phylogenetic analysis by maximum likelihood. Mol Biol Evol. 2007:24:1586–1591. https://doi.org/10.1093/molbev/msm088.
Zhang C, Rabiee M, Sayyari E, Mirarab S. ASTRAL-III: polynomial time species tree reconstruction from partially resolved gene trees. BMC Bioinformatics. 2018a:19:15–30. https://doi.org/10.1186/s12859-018-2129-y.
Zhang S-Q, et al. Evolutionary history of Coleoptera revealed by extensive sampling of genes and species. Nat Commun. 2018b:9:205. https://doi.org/10.1038/s41467-017-02644-4.

Associate editor: Christopher Wheat